



Cite this: *RSC Adv.*, 2019, 9, 38877

Received 19th October 2019
 Accepted 20th November 2019

DOI: 10.1039/c9ra08560b

rsc.li/rsc-advances

Highly selective synthesis of 2,5-bis(aminomethyl) furan *via* catalytic amination of 5-(hydroxymethyl) furfural with NH₃ over a bifunctional catalyst†

Hangkong Yuan,^a Bright T. Kusema,^{*b} Zhen Yan,^b Stéphane Streiff^b and Feng Shi^{ID} ^{*a}

The development of facile protocols for the selective synthesis of biomass-derived diamine is a highly desirable pursuit in the field of heterogeneous catalysis. Herein, a simple and highly efficient bifunctional CuNiAlO_x catalyst was developed for the one pot transformation of 5-(hydroxymethyl)furfural (5-HMF) into 2,5-bis(aminomethyl)furan (BAF) using a two-stage reaction process. Cu₄Ni₁Al₄O_x was found to be the most effective catalyst for this reaction, affording BAF in 85.9% yield. Our results could promote controllable conversion and utilization of biomass resource.

Amines are an important class of nitrogen-containing chemicals and are widely used in the synthesis of pharmaceuticals, agrochemicals, surfactants, dyes, polymers, and biologically active compounds.¹ Among the different amines, primary diamines are some of the most useful monomers for the production of polyamides and polyureas which were widely employed in everyday life including automotive, aerospace, electrical and electronics, building, and biomedicine industry.² Traditionally, they are produced from carbonyl and alcohol compounds which are derived from fossil resources. However, the depletion of fossil resources is a big concern as well as the environmental impact associated with their usage. Furthermore, there is a rising demand for biocompatible polymers to be used in industry, for example, in packaging and biomedicine. Therefore, the application of renewable resources to replace fossil resources for the production of primary diamines is highly desired.

Biomass as a renewable and ubiquitous resource is considered as the next generation feedstock for the chemical industry. Utilization of biomass as raw material has potential to replace diminishing fossil fuels with renewable feedstocks, thereby alleviating the dependence on petro-based materials, and reducing pollution.³ In addition, biomass-derived diamine monomers would meet the rising demand for biocompatible polymers. Therefore, the development of effective methods for the preparation of diamines from bio-based renewable

materials is an attractive prospect in view of establishing the sustainable development of societies.⁴ As one of the most important platform molecules derived from biomass, 5-(hydroxymethyl)furfural (5-HMF) is attracting increasing attention owing to the unique and versatile chemical structure containing both aldehyde and hydroxyl groups.⁵ 5-HMF could be used to synthesize 2,5-bis(aminomethyl)furan (BAF); however, selective synthesis of BAF from 5-HMF is a challenging task because the transformation is prone to form a series of by-products of secondary, tertiary and polymeric amine species.⁶ Thus, many multi-step routes were developed for the synthesis of BAF. Komanoya *et al.* developed a two-step method for the synthesis of BAF, in which 5-HMF was firstly converted into 5-(hydroxymethyl)furfurylamine (HMFA) over Ru/Nb₂O₅ catalyst and then converted into BAF over a homogenous [Ru(CO)ClH(PPh₃)₃] catalyst.⁷ Lin and co-workers have prepared BAF with 45.7% yield through the hydroxymethyl group of 5-HMF into amide group with CH₃CN by Ritter reaction, followed by reductive amination of aldehyde groups with NH₃ and hydrolysis of amide to primary amine⁸, Kim *et al.* reported the reductive amination of 2,5-diformylfuran to BAF over acid treated RANEY®-Ni catalysts with a yield of 42.6%.⁶ Xu and co-workers have demonstrated that BAF could be efficiently synthesized in 94.1% yield from hydrogenation of 2,5-diformylfuran dioxime which was generated from oximation of 2,5-diformylfuran (DFF).⁹ Compared to the above two or multi-steps methods, the direct amination of easily available 5-HMF to BAF would be advantageous with respect to atom efficiency and step economy. To date, however, only few catalytic systems dealing with direct transformation of 5-HMF into the BAF have been established. In 2018, an elegant method for the direct amination of 5-HMF with ammonia to BAF with 85% yield was achieved in the presence of homogeneous Ru/phosphine ligand complex.¹⁰ Recently, Wei and co-workers presented an effective

^aState Key Laboratory for Oxo Synthesis and Selective Oxidation, Lanzhou Institute of Chemical Physics (LICP), Chinese Academy of Sciences, Lanzhou 730000, China. E-mail: fshi@licp.cas.cn

^bEco-Efficient Products and Processes Laboratory (E2P2L), UMI 3464 CNRS-Solvay, 3966 Jin Du Road, Xin Zhuang Ind. Zone, 201108 Shanghai, China. E-mail: bright.kusema@solvay.com

† Electronic supplementary information (ESI) available. See DOI: 10.1039/c9ra08560b



8.6 mmol Na_2CO_3 and 1352.9 mmol NH_3 are the optimal amounts (Tables S2 and S3, ESI†). Na_2CO_3 act as a base to promote the hydrogen transfer reaction. It should be noted that the addition of excess NH_3 is indispensable to increase the selectivity towards the primary amine, thus achieving good BAF yield and mass balance. Furthermore, the impact of H_2 pressure was studied (Table S4, ESI†). Lower BAF yield and mass balance were obtained when H_2 pressure was reduced from 4.5 MPa to 3.0 MPa. H_2 shifts the equilibrium from imine to amine product, and also maintains the catalyst activity by avoiding carbonaceous deposits. Next, temperature screening of the second stage of the reaction showed that reducing the reaction temperature to 190 °C lowered the yield of BAF and substantially increased the yield of HMFA (2a), while raising the reaction temperature to 220 °C decreased mass balance (Table S5, ESI†). This observation suggests that 210 °C is the suitable temperature for the reaction. Investigation of the reaction time of first and second stage demonstrated that higher yield of 85.9% with 95.4% mass balance was afforded by prolonging the reaction time of first stage from 6 h to 9 h (Table 1, entry 8 and Tables S6 and S7, ESI†). It should be noted that HMFA was only produced after the first reaction stage, and the yield of BAF gradually increased to 75.2% after 18 h at the second stage, and remained constant even after prolonging the reaction time to 34 h. The above results clearly indicated that the reaction proceeded *via* reductive amination of aldehyde functional group of 5-HMF with NH_3 at 90 °C, followed by hydrogen-borrowing reaction of hydroxyl group with NH_3 at 210 °C. Finally, the $\text{Cu}_4\text{Ni}_1\text{Al}_4\text{O}_x$ is easily recovered by simple filtration and it could be used for three catalytic cycles without significant decline in catalytic performance, indicating the good stability of the catalyst (Table 1, entry 9). In order to figure out whether the reaction takes place homogeneously or heterogeneously, a leaching experiment was performed (Fig. S4†). After 2 h of reaction of HMF with NH_3 over $\text{Cu}_4\text{Ni}_1\text{Al}_4\text{O}_x$ at 210 °C and separating the solid catalysts, further reaction was operated on the residual liquids for another 16 h. Clearly, the reaction stopped after removing the solid catalyst. This observation demonstrates that the leached Cu and Ni should not be the active species.

The prepared catalytic samples were characterized by X-ray diffraction (XRD), transmission electron microscopy (TEM), X-ray photoelectron spectroscopy (XPS), and N_2 adsorption-desorption to reveal their structures. At first, XRD patterns of the different CuNiAlO_x catalysts were obtained to elucidate the crystal structures of the samples (Fig. 1).

The $\text{Cu}_1\text{Ni}_4\text{Al}_4\text{O}_x$ catalyst shows diffraction peaks at 36.9°, 43.5°, 63.2°, and 75.4°, which can be ascribed to the diffraction peaks of NiO(111), NiO(200), NiO(220), and NiO(311) (JCPDS card no: 47-1049). For the $\text{Cu}_1\text{Ni}_1\text{Al}_{1.6}\text{O}_x$, except for the diffraction peaks of the NiO, additional reflections are also visible at 38.9°, and 50.4°, which can be assigned to CuO(200) and Cu(200), respectively (CuO, JCPDS card no: 89-5899; Cu, JCPDS card no: 89-2838). With the increase of Cu : Al ratios in these catalysts, characteristic Cu(111), Cu(200), Cu(220), CuO(-111), CuO(200), and CuO(-202) reflections appearing at 43.2°, 50.4°, 74.1°, 35.6°, 38.9°, and 48.9°, respectively, were detected for

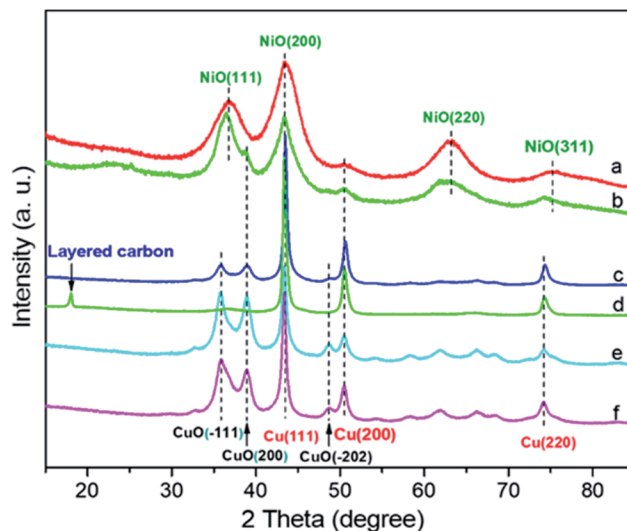


Fig. 1 XRD patterns of fresh and reused CuNiAlO_x catalysts. (a) $\text{Cu}_1\text{-Ni}_4\text{Al}_4\text{O}_x$, (b) $\text{Cu}_1\text{Ni}_1\text{Al}_{1.6}\text{O}_x$, (c) $\text{Cu}_4\text{Ni}_1\text{Al}_4\text{O}_x$, (d) reused $\text{Cu}_4\text{Ni}_1\text{Al}_4\text{O}_x$, (e) $\text{Cu}_6\text{Ni}_1\text{Al}_{5.6}\text{O}_x$, (f) $\text{Cu}_{19}\text{Ni}_1\text{Al}_{16}\text{O}_x$.

$\text{Cu}_4\text{Ni}_1\text{Al}_4\text{O}_x$, $\text{Cu}_6\text{Ni}_1\text{Al}_{5.6}\text{O}_x$, and $\text{Cu}_{19}\text{Ni}_1\text{Al}_{16}\text{O}_x$ (CuO, JCPDS card no: 89-5899; Cu, JCPDS card no: 89-2838). Moreover, there were no peaks observed for Ni species for $\text{Cu}_4\text{Ni}_1\text{Al}_4\text{O}_x$, $\text{Cu}_6\text{-Ni}_1\text{Al}_{5.6}\text{O}_x$, and $\text{Cu}_{19}\text{Ni}_1\text{Al}_{16}\text{O}_x$, which implied that the nickel species might be amorphous state or highly dispersed. Compared with fresh $\text{Cu}_4\text{Ni}_1\text{Al}_4\text{O}_x$, a new diffraction peak located at 18.0° indicating formation of the layered carbon (JCPDS card no: 50-1363) and disappearance of CuO phase were observed in $\text{Cu}_4\text{Ni}_1\text{Al}_4\text{O}_x$ catalyst reused for three times. Thus, we suppose that the Cu in CuNiAlO_x catalysts might promote the borrowing-hydrogen reaction but the role of CuO is still unclear¹⁴ and speculate that a slight loss of the catalytic activity could be attributed to formation of the layered carbon on the surface of $\text{Cu}_4\text{Ni}_1\text{Al}_4\text{O}_x$ catalyst.

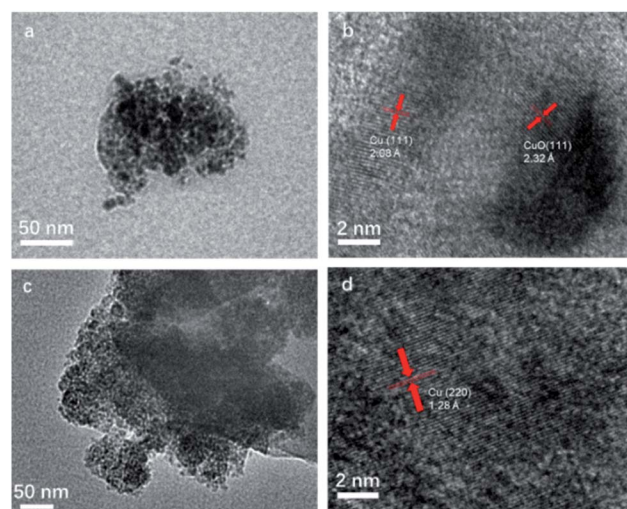


Fig. 2 TEM images of the catalysts. (a and b) $\text{Cu}_4\text{Ni}_1\text{Al}_4\text{O}_x$, (c and d) reused $\text{Cu}_4\text{Ni}_1\text{Al}_4\text{O}_x$.



The CuNiAlO_x catalysts were further characterized by TEM. Fig. S1† shows TEM micrographs of CuNiAlO_x. TEM analysis (Fig. 2) of the best Cu₄Ni₁Al₄O_x catalyst showed the formation of mainly Cu and Ni nanoparticles with sizes of 10–30 nm. The crystal lattices of Cu(111) and CuO(111) can be observed clearly in the magnified TEM micrographs. Compared with fresh Cu₄Ni₁Al₄O_x catalyst, the HRTEM images of the catalyst which was used three times showed that the crystal lattices of Cu(111) was maintained and the crystal lattices of CuO(111) was not observable, which are in good agreement with XRD results.

Furthermore, the surface composition of the CuNiAlO_x catalysts was analyzed by XPS. The XPS spectra of Cu 2p of fresh Cu₄Ni₁Al₄O_x is shown in Fig. 3a.

The XPS spectra of fresh Cu₄Ni₁Al₄O_x display two main peaks at 932.4 and 952.3 eV that can be attributed to Cu 2p_{3/2} and Cu 2p_{1/2} binding energies of Cu⁰ or Cu¹⁺. Considering that metallic copper was observed from XRD patterns and HRTEM image of the Cu₄Ni₁Al₄O_x catalyst, we suppose that binding energy of 932.4 eV might be assigned to the metallic copper. Other binding energies at 933.9 eV for Cu 2p_{3/2} and 953.9 eV for Cu 2p_{1/2} are ascribed to Cu²⁺. In addition to these peaks, shake-up satellite peaks were observed in the region of 940–945 eV (Cu 2p_{3/2}) and 959–965 eV (Cu 2p_{1/2}), also indicating the presence of Cu²⁺ species in Cu₄Ni₁Al₄O_x catalyst. According to XPS-peak-differentiation-imitating analysis, the ratio of Cu⁰/Cu²⁺ is 4.7 : 1. Fig. 3b shows Ni 2p spectra of Cu₄Ni₁Al₄O_x catalysts. The peaks of the Ni 2p XPS spectrum at 855.4 eV (Ni 2p_{3/2}) and 856.7 eV (Ni 2p_{1/2}) were in accordance with NiO. Besides these peaks, shake-up satellite peaks were observed in the region of 857–865 eV (Ni 2p_{3/2}) and 877–884 eV (Ni 2p_{1/2}). Additional spectra for the other catalysts can be found in the ESI (Fig. S2†).

The N₂ adsorption–desorption tests (Fig. S3, ESI†) showed that the BET surface areas of the Cu₁Ni₄Al₄O_x, Cu₁Ni₁Al_{1.6}O_x, Cu₄Ni₁Al₄O_x, Cu₆Ni₁Al_{5.6}O_x, Cu₁₉Ni₁Al₁₆O_x, Cu₁Al₁O_x and Ni₁-Al₄O_x were 202.39, 169.75, 101.16, 83.35, 68.16, 79.77, and 326.21 m² g⁻¹, respectively (Table S8, ESI†). Therefore, the high selectivity of Cu₄Ni₁Al₄O_x should not be attributed solely to its high surface area. It can be inferred that the good catalytic performance of Cu₄Ni₁Al₄O_x catalyst in the direct amination of HMF to desired BAF product is attributed to bulk Cu and highly dispersed Ni species for the dehydrogenation and hydrogenation properties, respectively.

In conclusion, we have successfully developed an efficient methodology for highly selective synthesis of biomass-derived

BAF *via* direct amination of 5-HMF with NH₃ over bifunctional CuNiAlO_x catalyst using two-stage reaction process. By tuning the Cu/Ni molar ratio, Cu₄Ni₁Al₄O_x exhibited excellent catalytic performance in the direct amination of 5-HMF to BAF, affording the desired product in 85.9% yield. Experimental results suggested that the reaction proceeded *via* reductive amination of aldehyde group of 5-HMF with NH₃ at 90 °C, followed by hydrogen-borrowing reaction of hydroxyl of 5-HMF with NH₃ at 210 °C. This work offers an effective methodology for the controlled synthesis of biomass-derived diamines monomers.

Conflicts of interest

There are no conflicts to declare.

Acknowledgements

Financial supports from NSFC (21802147), the Youth Innovation Promotion Association (2019409), “Light of West China” Program and Fujian Innovation Academy of CAS are gratefully acknowledged. Solvay is gratefully acknowledged for funding.

Notes and references

- (a) E. Karsten, H. Erhard, R. Roland and H. Hartmut, *Amines, Aliphatic in Ullmann's Encyclopedia of Industrial Chemistry*, Wiley-VCH, Weinheim, 2005; (b) A. Ricci, *Amino group chemistry: from synthesis to the life sciences*, John Wiley & Sons, 2008.
- (a) D. K. Chattopadhyay and K. V. S. N. Raju, *Prog. Polym. Sci.*, 2007, **32**, 352–418; (b) J. M. García, F. C. García, F. Serna and L. D. L. P. José, *Prog. Polym. Sci.*, 2010, **35**, 623–686.
- (a) A. Corma, S. Iborra and A. Velty, *Chem. Rev.*, 2007, **107**, 2411–2502; (b) D. Li, W. Ni and Z. Hou, *Chin. J. Catal.*, 2017, **38**, 1784–1793.
- (a) I. Delidovich, P. J. Hausoul, L. Deng, R. Pfitzenreuter, M. Rose and R. Palkovits, *Chem. Rev.*, 2016, **116**, 1540–1599; (b) V. Froidevaux, C. Negrell, S. Caillol, J. P. Pascault and B. Boutevin, *Chem. Rev.*, 2016, **116**, 14181–14224; (c) M. Pelckmans, T. Renders, S. Van de Vyver and B. F. Sels, *Green Chem.*, 2017, **19**, 5303–5331; (d) M. Pera-Titus and F. Shi, *ChemSusChem*, 2014, **7**, 720–722.
- (a) P. Pal and S. Saravanamurugan, *ChemSusChem*, 2019, **12**, 145–163; (b) H. Yuan, J.-P. Li, F. Su, Z. Yan, B. T. Kusema, S. Streiff, Y. Huang, M. Pera-Titus and F. Shi, *ACS Omega*, 2019, **4**, 2510–2516; (c) F. Gao, J. Chen, Z. Huang and C. Xia, *J. Mol. Catal.*, 2018, **32**, 276–293.
- N.-T. Le, A. Byun, Y. Han, K.-I. Lee and H. Kim, *Green Sustainable Chem.*, 2015, **05**, 115–127.
- T. Komanoya, T. Kinemura, Y. Kita, K. Kamata and M. Hara, *J. Am. Chem. Soc.*, 2017, **139**, 11493–11499.
- X. Wang, W. Chen, Z. Li, X. Zeng, X. Tang, Y. Sun, T. Lei and L. Lin, *J. Energy Chem.*, 2018, **27**, 209–214.
- Y. Xu, X. Jia, J. Ma, J. Gao, F. Xia, X. Li and J. Xu, *Green Chem.*, 2018, **20**, 2697–2701.

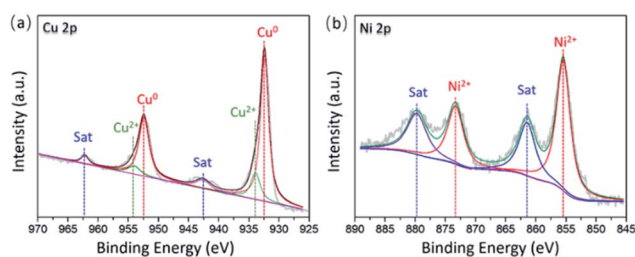


Fig. 3 XPS spectra of (a) Cu 2p core level and (b) Ni 2p core level for Cu₄Ni₁Al₄O_x.



- 10 D. Pingen, J. B. Schwaderer, J. Walter, J. Wen, G. Murray, D. Vogt and S. Mecking, *ChemCatChem*, 2018, **10**, 3027–3033.
- 11 K. Zhou, H. Liu, H. Shu, S. Xiao, D. Guo, Y. Liu, Z. Wei and X. Li, *ChemCatChem*, 2019, **11**, 2649–2656.
- 12 K.-I. Shimizu, *Catal. Sci. Technol.*, 2015, **5**, 1412–1427.
- 13 X. Cui, X. Dai, Y. Deng and F. Shi, *Chem.–Eur. J.*, 2013, **19**, 3665–3675.
- 14 (a) J. Aston, T. Peterson and J. Holowchak, *J. Am. Chem. Soc.*, 1934, **56**, 153–154; (b) T. Yamakawa, I. Tsuchiya, D. Mitsuzuka and T. Ogawa, *Catal. Commun.*, 2004, **5**, 291–295; (c) Y. Wu, H. Huang, X. Dai and F. Shi, *ChemSusChem*, 2019, **12**, 3185–3191.

